DOI: 10.1021/ma902396n

Macromolecules
ARTICLE

Conformationally Twisted Semiconducting Polythiophene Derivatives with Alkylthiophene Side Chain: High Solubility and Air Stability

Jong Won Park,[†] Dong Hoon Lee,[‡] Dae Sung Chung,[‡] Dong-Min Kang,[†] Yun-Hi Kim,*[,§] Chan Eon Park,*[,‡] and Soon-Ki Kwon*[,†]

[†]*School of Materials Science and Engineering and ERI, Gyeongsang National University, Jinju 660-701, Korea,* [‡]*Organic Electronics Laboratory, Department of Chemical Engineering, Pohang University of Science and Technology, Pohang 790-784, Korea, and* [§]*Department of Chemistry and RINS, Gyeongsang National University, Jinju 660-701, Korea*

Received October 30, 2009; Revised Manuscript Received February 2, 2010

ABSTRACT: We report the synthesis of polythiophene derivatives that contain decylthiophenyl side chains, using synthetic strategies that achieve high organic semiconductor field effect mobilities by enhancing the π-conjugation in the side-chain conjugated system. With increased charge densities, we obtained high field effect mobilities, up to 0.050 and 0.003 $cm^2/(V\ s)$ from poly(3,4‴-di(decylthiophenyl) sexithiophene) (PDTST) and poly(3,4‴-di(decylthiophenyl) quaterthiophene) (PDTQT), respectively. PDTQT and PDTST are characterized by UV−vis, DSC, AFM images, and GIXD patterns. Increased conformational rotation in the main backbone, caused by intramolecular repulsion between neighboring thiophene units, lowers the HOMO level and introduces remarkable chemical stability in the presence of air as well as increases processability due to high solubility. The high solubility and oxidative stability of PDTST and PDTQT indicate that these side-chain conjugation system strategies have the potential for improving other thiophene-based semiconducting polymers.

Introduction

Polymeric organic semiconductors have been extensively studied for several years. Among them, conjugated polythiophenes (PTs) are one of the most promising materials because of their good solubility as well as high electrical performance.[1] Despite these good characteristics, PT-based organic field effect transistors (OFETs) have some disadvantages that hinder their use as replacements for Si transistors; for example, they have low field effect mobilities, high off-currents, poor oxidative stabilities, and low uniformity.[2] To overcome these limitations, a wide range of structural modifications has been tried, focusing particularly on the control of the effective length of conjugation to achieve a balance between sufficient π-conjugation, which yields a high field effect mobility, and nonexcessive conjugation, which yields strong resistance to oxidative doping. Regioregular P3HT thin films have been shown to have a lamellar structure with a high coplanarity and rigidity of the polymer backbone, induced by side-chain substitutions at each thiophene unit. High coplanarity can result in both highly delocalized π-conjugation along the main backbone and a 2D lamellar structure with strong interchain stacking. Although high crystallinity and a field effect mobility of 0.1 $cm^2/(V\ s)$ may be attributed to coplanarity, coplanarity also introduces susceptibility to photoinduced oxidative doping.[2] Recently, Ong et al.[3] reported that poly(3,3‴-dialkylquaterthiophene) (PQT), which has two unsubstituted thienyl moieties between each alkyl-substituted thiophene ring, is characterized by increased torsional deviations resulting in improved oxidative stability. Although the specific mechanisms are different, fluorene and thienothiophene blocks were deployed between thiophene units in the main backbones of poly(9,9′-*n*-dioctylfluorene-alt-bithiophene) (F8T2) and poly(2,5-bis(3-dodecyl-thiophene-2-yl)thieno[3,2-*b*]thiophene) (PBTTT) to cut down the intramolecular conjugation to several repeating units and finally to obtain increased oxidative stability.[4] Two polymers also successfully showed high field effect mobilities of up to 0.02 (F8T2) and 0.7 $cm^2/(V\ s)$ (PBTTT), which means they were in a good balance on the control of the intramolecular conjugation.[4] Poly(2,5-bis(2-thienyl)-3,6-dialkylthieno[3,2-*b*]thiophene) (PTAT), which allows for more conformational rotation of the thienyl units compared with PBTTT, also showed a high mobility of 0.25 $cm^2/(V\ s)$ with a much lower highest-occupied molecular orbital (HOMO) level.[5]

In addition to the introduction of structural modifications to the main chain, there also have been some efforts to change the structure of the side chains.[6] Regioregular P3HT with chiral alkyl side chains, bulky side chains, and carboxylic side chains were reported to yield poor electrical performances because of hindered self-organization by the side chains.[6a] Hou et al.[7a] introduced phenylene vinyl moieties into the side chains of a thiophene backbone polymer with the intention of inducing extended π-conjugation in the side chains. This conjugated side chain system may guarantee strong intermolecular interactions as a result of the extension of electron delocalization through the side chain, similar to the delocalization present in the main backbone. Because of the high coplanarity and extended π-conjugation induced by the vinylene unit, Hou et al. reported that poly[3-(5-octyl-thienylene-vinyl)-thiophene] (POTVT) films revealed higher HOMO levels and a small bandgap of 1.77 eV, which were advantageous for the absorption cross-section of organic photovoltaics but introduced crucial weaknesses in the stability of organic thin film transistors (OTFTs).[7] Recently, poly(3,3″-hexylated-thiophenyl terthiophene) and poly(3,3″-hexylated-bithiophenyl terthiophene) were also reported to yield small

*Corresponding authors. (Y.-H.K.) Tel: +82-55-751-6016. Fax: +82-55-761-0244. E-mail: ykim@gnu.ac.kr. (C.E.P.) Tel: +82-54-279-2269. Fax: +82-54-279-8298. E-mail: cep@postech.ac.kr. (S.-K.K.) Tel: +82-55-751-5296. Fax: +82-55-753-6311. E-mail: skwon@gnu.ac.kr.

 Published on Web 02/09/2010

bandgaps of 1.98 of 1.77 eV, with 2.5% power conversion efficiencies in polymer-based solar cells and relatively low field effect mobilities of 3.5×10^{-4} to 4.6×10^{-3} because of the backbone distortion introduced by too many alkyl-thiophene side chains.[8]

Here we designed poly(3,4‴-di(decylthiophenyl) quaterthiophene)) (PDTQT) and poly(3,4‴-di(decylthiophenyl) sexithiophene) (PDTST) for use in high-performance OTFTs to increase the π-electron density per repeating unit and lower the HOMO level. PDTQT contains two unsubstituted thienyl moieties between each decylthiophene-substituted thiophene ring. PDTST structure alternates between two and four unsubstituted thienyl moieties between each decylthiophene-substituted thiophene ring. Both PDTQT and PDTST have high π-electron densities per repeating unit compared with the reported PQT derivatives. It is also expected that the oxidative stabilities of PDTQT and PDTST are increased, not only because these polymers avoid excessive π-conjugation by the insertion of unsubstituted thienyl moieties in the main backbone chain but also because the backbone distorts through the sulfur interactions between decylthiophene side chains and adjacent unsubstituted core thiophenes in the main backbone. It is possible that intramolecular repulsion, induced by the electronegative sulfur atoms, could introduce additional torsional distortion and curtail the π-conjugation along the main backbone. UV−vis absorption spectra and cyclic voltammetry indicated that the HOMOs of both polymers were lower than those of other well-known semiconducting polymers. The OTFT fabricated using PDTST, with a lower density side chain, showed a much higher field effect mobility of 0.050 $cm^2/(V\ s)$ than the field effect mobility of PDTQT (0.003 $cm^2/(V\ s)$). Moreover, the polymers' high electrical characteristics were stable over the course of 30 days of exposure to air; even after 90 days, the field effect mobilities of the polymers were measured at $>80\%$ initial values.

Synthesis

2-Decylthiophene. 2-Decylthiophene was synthesized according to published procedures with a yield of 79%, producing a colorless oil with bp 120 °C at 0.6 Torr. ^{1}H NMR (300 MHz, $CDCl_3$, δ): 7.17−7.15 (m, 1H), 6.99−6.96 (m, 1H), 6.85−6.84 (m, 1H), 2.92−2.87 (t, 2H), 1.76−1.71(m, 2H)1.5−1.2 (m, 14H), 0.99−0.95 (t, 3H)

2-Bromo-5-decylthiophene. *N*-Bromosuccinimide (NBS) (26 g, 147 mmol) was added to the solution of 2-decylthiophene (30 g, 137 mmol) in $CHCl_3$ and acetic acid (1:1, 200 mL) at 0 °C. The reaction mixture was stirred for 2 h at room temperature and added to a 1 M NaOH aqueous solution. After extraction with methylene dichloride, the organic layer was removed and dried over magnesium sulfate. The product was obtained by distillation, bp 160 °C at 0.6 Torr. ^{1}H NMR (300 MHz, CDCl, δ):6.9−6.8 (d, 1H), 6.56−6.55 (d, 1H), 2.79−2.72 (t, 2H), 1.7−1.6(m, 2H), 1.5−1.2 (m, 14H), 0.99−0.95 (t, 3H)

5-Decyl-2,3′-bithiophene. Mg (1.64 g, 67.47 mmol) was activated in ether, 2-bromo-5-decylthiophenethiophene (20.46 g, 67.47 mol) was added, and the reaction was stirred for 3 h. 3-bromothiophene (10 g, 61.33 mol) and Ni(dppf)Cl_2 were added to the mixture at 0 °C. After being stirred for 12 h at room temperature, the reaction was quenched with water and extracted with methylene dichloride. The crude product was purified by column chromatography, eluted with hexane, then recrystallized from MeOH. Yield: 13 g, 72%. ^{1}H NMR (300 MHz, $CDCl_3$, δ): aromatic (C−H), 7.38−7.33 (m, 3H), 7.08−7.07 (d, 1H), 6.78−6.76 (d, 1H), aliphatic (C−H) 2.9−2.8 (t, 2H), 1.8−1.3 (m, 2H), 1.4−1.3 (m, 14H), 1.0−0.9 (t, 3H).

2′-Bromo-5-decyl-2,3′-bithiophene. 5-Decyl-2,3′-bithiophene (5 g, 16.31 mmol) was dissolved in 50 mL of dimethylformamide (DMF). NBS was added to the solution at 0 °C, and the mixture was stirred for 2 h at room temperature. The reaction was quenched with water and extracted with ether. The crude product was purified by column chromatography and eluted with hexane. Yield: 5.9 g, 94%.

^{1}H NMR (300 MHz, $CDCl_3$, δ): aromatic (C−H), 7.32−7.31 (d, 1H), 7.27−7.25 (d, 1H), 7.14−7.12 (d, 1H), 6.80−6.79 (d, 1H), aliphatic (C−H) 2.88−2.83 (t, 2H), 1.77−1.72 (m, 2H), 1.42−1.32 (m, 14H), 0.96−0.92 (t, 3H).

3-(5-Decylthiophene-2-yl)-2-(5-(5-(3-(5-decylthiophene-2-yl)thiophene-2-yl)thiophene-2-yl)thiophene (DDT). 2′-Bromo-5-decyl-2,3′-bithiophene (6.5 g (16.86 mmol)) and 3.32 mL (6.75 mmol) of 5,5′-bis(tributylstannyl)-2,2′-bithiophene were dissolved in toluene. After degassing, 0.23 g (0.2 mmol) $Pd(PPh_3)_4$ was added to the solution, which was stirred at 100 °C for 24 h. The reaction mixture was extracted with methylene dichloride. The crude product was purified by column chromatography and eluted with hexane. Yield: 2.3 g, 49% ^{1}H NMR (300 MHz, $CDCl_3$, δ): aromatic (C−H), 7.28−7.25 (m, 2H), 7.15−7.13 (d, 2H), 7.05−7.02 (m, 4H), 6.92−6.91 (d, 2H), 6.70−6.69 (d, 2H), aliphatic (C−H) 2.83−2.78 (t, 4H), 1.72−1.63 (m, 4H), 1.37−1.27 (m, 28H), 0.91−0.87 (t, 6H).

5-Bromo-2-(5-(5-(5-bromo-3-(5-decylthiophene-2-yl)thiophene-2-yl)thiophene-2-yl)-3-(5-decylthiophene-2-yl)thiophene (BDDT). NBS (0.25 g, 1.42 mmol) was slowly added to the mixture of DDT (0.5 g, 0.64 mmol), which was dissolved in DMF at 0 °C. After the mixture was stirred for 5 h, the reaction was terminated by the addition of 2 M HCl. The organic layer was extracted with ether and dried over $MgSO_4$. The crude product was purified by column chromatography, eluted with hexane, and recrystallized from acetone. Yield: 0.4 g, 68%. ^{1}H NMR (300 MHz, $CDCl_3$, δ): aromatic (C−H), 7.28−7.25 (m, 2H), 7.28 (2, 2H), 7.1−6.98 (m, 4H), 6.89−6.88 (d, 2H), 6.69−6.67 (d, 2H), aliphatic (C−H) 2.81−2.76 (t, 4H), 1.72−1.62 (m, 4H), 1.36−1.27 (m, 28H), 0.92−0.87 (t, 6H).

Poly(3,4‴-di(decylthiophenyl) sexithiophene) (PDTST). BDDT (1 g, 1.07 mmol) and 5,5′-bis(tributylstannyl)-2,2′-bithiophene (0.53 g, 1.07 mmol) were dissolved in toluene (30 mL). After degassing, $Pd(PPh_3)_4$ was added to the mixture and stirred for 48 h at 80 °C. Subsequently, 2-bromonaphtalene was injected to the reaction mixture with a small amount of catalysts for end-capping, and the reaction was stirred for 6 h. After precipitation from chloroform/methanol, the desired polymer was obtained. Yield: 60%. ^{1}H NMR (300 MHz, $CDCl_3$, δ): aromatic (C−H), 7.1−6.8 (br, 14H), aliphatic (C−H), 2.7 (br, 4H), 1.6−0.9 (br, 38H).

Poly(3,4‴-di(decylthiophenyl) quaterthiophene) (PDTQT). DMF (5 mL) and toluene (3 mL) were added to the mixture of Ni(COD) (0.44 g, 1.61 mmol), COD (0.17 g, 1.61 mmol), and BPY (0.25 g, 1.61 mmol) at 60 °C under a nitrogen atmosphere. Subsequently, 0.5 g (0.54 mmol) of BDDT dissolved in 20 mL of dried toluene was added, and the reaction was maintained at 80 °C for 48 h. 2-Bromonaphtalene was injected to the reaction mixture with small amount of catalysts for end-capping, and the reaction was stirred for 6 h. After precipitation from chloroform/methanol, the desired polymer was obtained. Yield: 50%. ^{1}H NMR (300 MHz, $CDCl_3$, δ): aromatic (C−H), 7.5−6.5 (br, 10H), aliphatic (C−H), 3.0−2.5 (br, 4H), 1.5−0.5 (br, 38H).

Results and Discussion

The syntheses of PDTQT and PDTST are described in Scheme 1. 5-Decyl-2,3′-bithiophene was prepared from 2-bromo-5-decylthiophene and 3-bromothiophene by the Grignard reaction with good yields. Stille coupling of 2-bromo-5′-decyl-2′,3-bithiophene to 5,5′-bis(tributylstannyl)-2,2′-bithiophene, followed by bromination, gave monomer **1**. Subsequent dehalogenative

Scheme 1. Synthetic Routes of PDTST and PDTQT

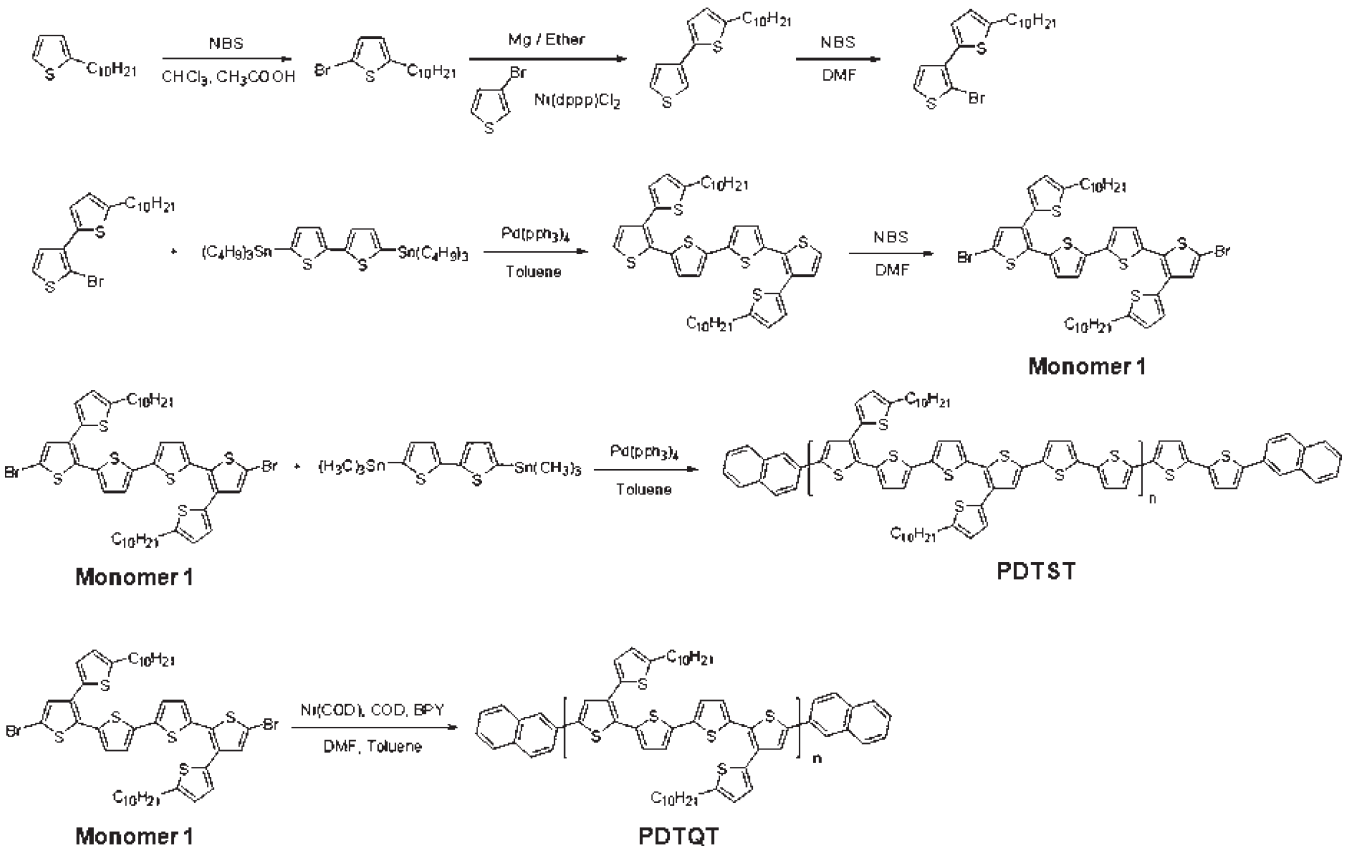

coupling polymerization, for the synthesis of PDTQT, was carried out in the presence of a slight excess of $Ni(COD)_2$ (COD: 1,5-cyclooctadiene) and a catalytic amount of 2,2′-dipyridyl, with refluxing in toluene and DMF (1:1). PDTST was synthesized from the Stille coupling of monomer 1 to bis-(tributylstannyl)-2,2′-bithiophene in the presence of $Pd(PPh_3)_4$ in toluene at 80 °C. The 2-bromonaphthalene was injected in the reaction mixture of polymerizations with end-capping reagent. The end-capping of terminal thiophene groups is expected to prevent oxidation of the generated radical cations.[9] The obtained polymers were purified by multiple precipitation and Soxhlet extractions, which afforded the final polymers as orange-red solids. PDTQT and PDTST showed high solubility in common organic solvents such as chloroform, methylene chloride, and toluene, whereas many semiconducting polymers for OFET showed limited solubility. This high solubility, which is very important for the practical application of OFET, might come from the slightly twisted conformation by introduction of decylthiophene. Gel permeation chromatography (GPC) analysis determined the number-average molecular weight (M_n) to be 12 700 with a polydispersity index of 1.68 for PDTQT and M_n = 7500 with a polydispersity index of 1.48 for PDTST, against polystyrene standards.

Figure 2 shows the UV−vis absorption and PL spectra of PDTQT and PDTST both in chloroform solution and in the film state. The obtained PDTQT and PDTST showed a broad absorption band. The side chain $\pi \rightarrow \pi^*$ transitions appeared near 300 nm for both PDTST and PDTQT, whereas the conjugated main chain $\pi \rightarrow \pi^*$ transitions appeared at 540 and 507 nm in the film state and 493 and 472 nm in solution, respectively. PDTQT exhibited a higher energy absorption maximum at 472 nm compared with 493 nm for PDTST, even though PDTQT had a much more densely conjugated side chain. This observation suggests that intramolecular conjugation of PDTQT may be

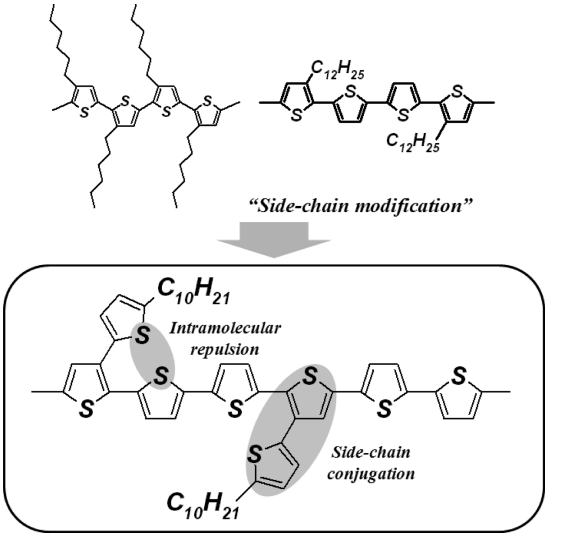

Figure 1. Schematic structure of the side chain conjugation polymer.

hindered by conformational distortions of the main backbone because of the presence of the side chains. For both polymers, a relatively small red shift of 40 nm in the absorption spectra, upon going from the solution to the thin-film state, was observed, in contrast with the observation of a large red shift of the regioregular P3HT (100 nm) and PQT (75 nm). The red shift from solution to film was also observed in the PL spectra of PDTQT and PDTST (PDTST, 67 nm; PDTQT, 58 nm). In UV−visible spectra, a vibronic absorption shoulder at 610 nm, indicative of an ordered microcrystalline polymer structure, was weakly observed in PDTST but not in PDTQT.[10] Therefore, both PDTST and PDTQT appeared to form low crystallinity, nearly

amorphous film structures. This conclusion was also supported by atomic force microscopy (AFM) images, grazing incidence X-ray diffraction (GIXD) patterns, and differential scanning calorimetry (DSC) curves. The polymers' optical and electrochemical properties are summarized in Table 1.

The HOMO levels of PDTST and PDTQT were determined from the cyclic voltammograms (vs Ag/AgCl) illustrated in Figure 3. From the onset of the oxidation potentials, each HOMO level was calculated from the equation, $E_{HOMO} = -(E_{on}^{ox} + 4.4)$. As shown in Table 1, relatively low HOMO levels of −5.21 and −5.27 eV were measured, which could be explained by the presence of conformational distortion enhanced by intramolecular repulsion. Unsubstituted core thienyl moieties in each repeating unit of the polymer chain allowed additional torsional deviation relative to most planar polymers, for example, regioregular P3HT(−4.8 eV).[11b] In addition, the interaction between electronegative sulfur atoms in the decylthiophene side chains and in most adjacent unsubstituted core thiophenes is expected to increase these deviations, as depicted in Figure 1. Considering that the lower HOMO level of polymer generally engenders higher oxidative stability, the curtailed intramolecular π-conjugation along the main backbone can be expected to give better air-stability of resulting devices.

Structural analysis by GIXD and AFM were obtained to investigate the molecular ordering and film morphology of these polymers. GIXD analysis was performed at the 10C1 beamline (wavelength, 1.54 Å) of the Pohang Accelerator Laboratory (PAL). Each film was prepared by spin coating the polymer onto a Si/SiO_2 substrate modified by octyltrichlorosilane (OTS) to develop a molecular ordering similar to that of FET devices. Figure 4 shows the out-of plane GIXD pattern. Each sample exhibited obvious diffractions at $2\theta = 3.35°$ (PDTST) and 3.6° (PDTQT), which corresponded to interlayer d spacings of 26.34 and 24.18 Å, respectively. By comparison with the interlayer d spacings of other polymers containing side chains of similar length to the polymers discussed here, for example, PQT-12 (18.5 Å) and regioregular poly(3-dodecylthiophene) (27.2 Å), the PDTST and PDTQT polymers appeared to self-assemble into crystalline structures via intermolecular side chain end-to-end interactions instead of by a side-chain interdigitated structure.[3,11] This mechanism may be favored by the bulky pendant side chains, which can limit polymer chain mobility during self-assembly. Another diffraction center was detected near $2\theta = 20.5°$, in a direction parallel to the substrate. (See Figure S2 in the Supporting Information.) This second diffraction center corresponded to a $\pi-\pi$ stacking distance of 4.3 Å, which is a relatively long distance for charge carrier transport compared with 3.8 Å for PQT and regioregular P3HT.[3,11] This observation supports the conclusion that PDTST and PDTQT experience

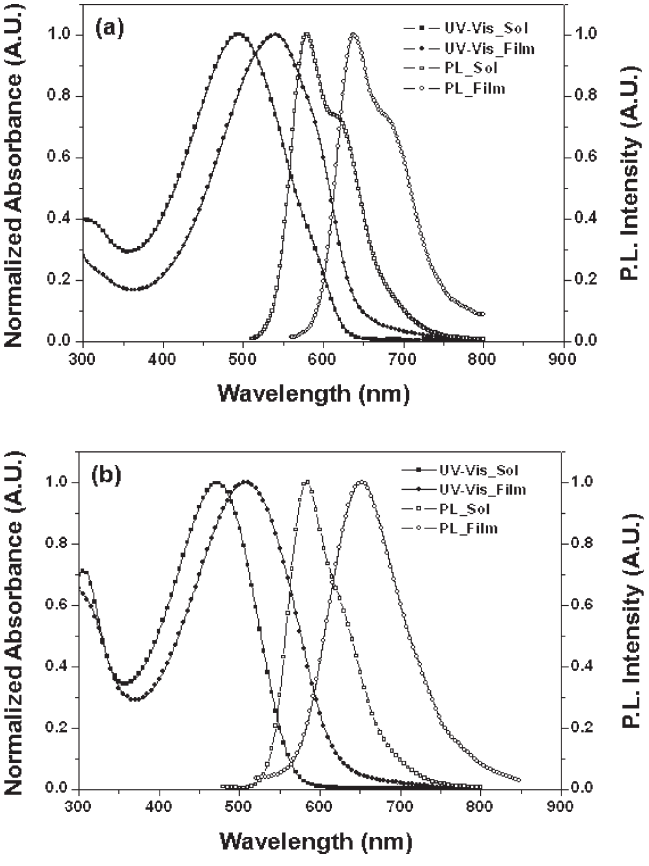

Figure 2. UV−vis absorption and PL spectra for PDTST and PDTQT in chloroform solutions and in the film state.

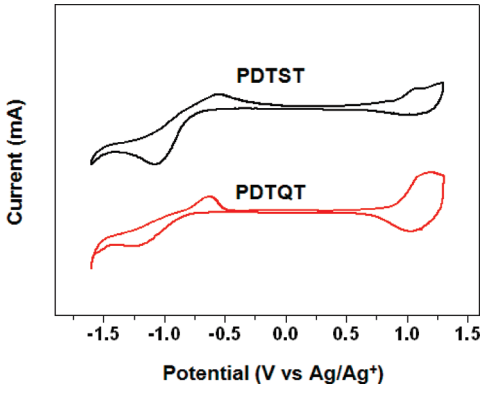

Figure 3. Cyclic voltammograms for PDTST and PDTQT films.

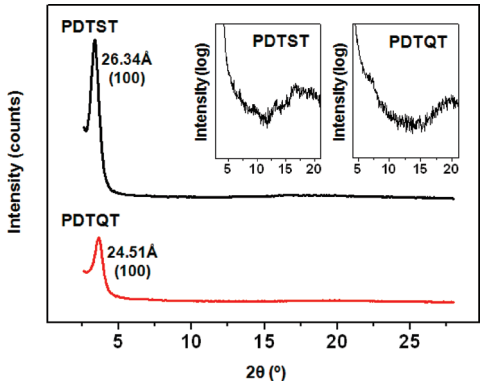

Figure 4. Out-of-plane GIXD patterns for PDTST and PDTQT spin-coated onto ODTS-pretreated dielectric surfaces (inset: the same patterns on the log scale).

Table 1. Optical and Electrochemical Properties of PDTST and PDTQT

	optical properties				electrochemical properties					
polymer	UV λ_{max}^{sol} (nm)	UV λ_{max}^{film} (nm)	PL λ_{max}^{sol} (nm)	PL λ_{max}^{film} (nm)	E_g^{opt} (eV)	$E_{1/2}^{ox}$ (eV)	E_{HOMO} (eV)	$E_{1/2}^{red}$ (eV)	E_{LUMO} (eV)	E_g^{ec} (eV)
PDTST	493	540	585	652	1.94	0.86	−5.21	−0.79	−3.61	1.65
PDTQT	472	507	580	638	2.01	0.92	−5.27	−0.83	−3.57	1.75

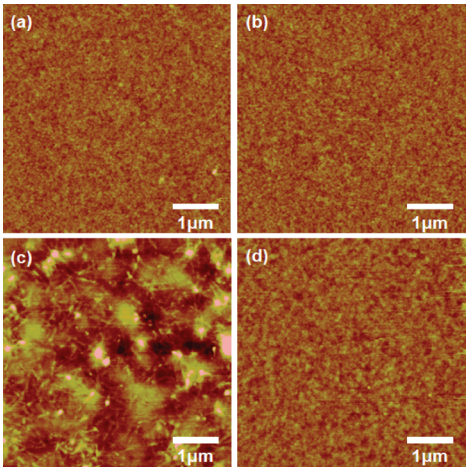

Figure 5. Atomic force microscopy height images for (a) as-spun films of PDTST, (b) as-spun films of PDTQT, (c) films of PDTST that had been thermally annealed at 100 °C, and (d) films of PDTQT that had been thermally annealed at 100 °C.

more torsional deviations than other semiconducting polymers, which may pose an obstacle to superior device performance. However, in terms of processability, this longer $\pi-\pi$ stacking distance can be a great merit because high solubility could be achieved despite the low density of side chain substitution. As shown in the GIXD pattern, PDTST was more crystalline than PDTQT, which displayed an isotropic nodular morphology in AFM imaging (Figure 5), even after thermal annealing. In sharp contrast, the morphology of PDTST changed from a nodule-like structure to a structure of higher crystallinity, after thermal annealing, by developing fibril crystalline domains. It is likely that a more distorted conformation of PDTQT would hinder the effective packing of polymer chains in the $\pi-\pi$ stacking direction.

Time-of-flight (TOF) photocurrent measurements were performed to study the bulk transport properties of PDTST and PDTQT. The TOF devices were prepared by drop-casting each polymer, dissolved in a 1 wt % chloroform solution, onto a transparent indium tin oxide (ITO)-coated glass. Onto the 8 μm polymer film (measured by a surface profiler, Alpha step 500, Tencor), a thin Al layer was deposited as the top electrode. Figure 6d depicts the current−voltage ($I-V$) characteristics under varying electric field strength. As the bias applied to the device varied from 200 to 500 V, the drift mobility at 2.5×10^{-4} cm^2/(V s) could be calculated from the equation $\mu = d/Et_{tr}$, where d is the thickness of the film, E is the applied electric field on the device, and t_{tr} is the photocurrent transient time measured from the kinks shown in Figure 6d.[12] From this value, which was very similar to that of regioregular P3HT (2×10^{-4} cm^2/(V s)), the PDTST and PDTQT polymers were determined to be sufficiently good hole transport materials.[12]

The thin film transistor (TFT) performance was characterized using a bottom-gate top-contact device geometry. Onto the heavily n-doped Si/SiO_2 substrate, spin-coated films of PDTST and PDTQT were prepared using *p*-xylene (PDTST) and chloroform (PDTQT) as solvents. Between the substrate and polymer film, a variety of surface modifications were preintroduced; for example, pretreatment with octadecyltrichlorosilane (ODTS), octyltrichlorosilane (OTS), and hexamethyldisilazane (HMDS) produced a hydrophobic dielectric surface with more edge on structure of polymer chain. The source and drain electrodes were thermally evaporated (to a thickness of 100 nm) through a shadow mask, yielding channel widths and lengths of 1500 and 150 μm, respectively. Field effect mobilities were measured in the saturation regime using the relationship $\mu_{sat} = (2I_{DS}L)/(WC(V_g - V_{th})^2)$, where I_{DS} is the saturation drain current, C is the

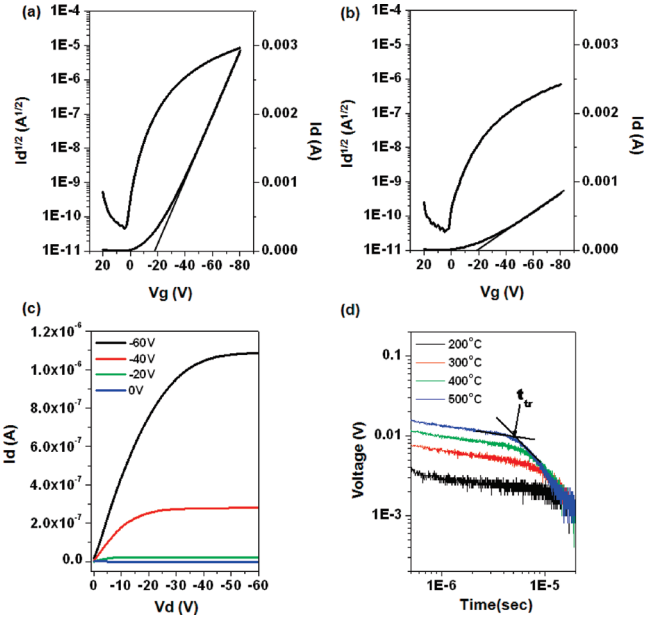

Figure 6. Field effect transistor device characteristics under ambient air with PDTST and PDTQT semiconductors: Transfer characteristics of (a) PDTST and (b) PDTQT, (c) Output characteristics of PDTST, and (d) time-of-flight photocurrent transients of PDTST.

Table 2. OFET Device Characteristics for PDTST and PDTQT

polymer	surface modification	mobility (cm^2/(V s))	threshold voltage (V)	on/off ratio
PDTST	ODTS	5.1×10^{-2}	−7.9	10^5
	OTS	2.6×10^{-2}	−11.9	10^4
	HMDS	1.8×10^{-2}	−14.7	10^4
	bare	7.3×10^{-3}	−5.5	5×10^3
PDTQT	ODTS	3.0×10^{-3}	−16.8	10^3
	OTS	6.3×10^{-4}	−14.8	10^3
	HMDS	1.7×10^{-4}	−8.6	10^3
	bare	3.7×10^{-5}	−3.1	10^2

capacitance of the oxide dielectric, V_g is the gate bias, and V_{th} is the threshold voltage. The mobilities and on/off ratios of the two polymers are summarized in Table 2. Highly crystalline PDTST was found to yield an electrical performance that was superior to that of the low-crystalline PDTQT. As shown in Figure 6a,b, PDTST revealed typical transfer curves, a highest saturation mobility of 0.025 cm^2/(V s), and an on/off ratio of 10^5, from the ODTS-pretreated device. PDTQT exhibited a one-order-of-magnitude-lower hole mobility of 0.003 cm^2/(V s) and an on/off ratio of 5×10^3. Thermal annealing at 100 °C for 30 min raised the hole mobility of PDTST to 0.050 cm^2/(V s). In contrast, thermal annealing afforded a worse device performance for PDTQT. The increased mobility of PDTST may have resulted from the increased degree of crystallinity produced by thermal annealing, as verified by AFM and GIXD. PDTQT polymer chains were thought to be incapable of developing crystalline domains during thermal treatment because of the density of the bulky side chains and the substantially distorted conformation of the polymer backbone. Additionally, better device performance was observed for the more hydrophobic surfaces, such as ODTS, and OTS, as shown in Figure S3 of the Supporting Information.

We tested the oxidation stability of our FET devices. Prepared devices were pretreated with ODTS and were not thermally annealed. Stability tests were performed under ambient air (~40% humidity) conditions in the dark for 1 month, and the electric characteristics were subsequently measured. To make reliable results, regioregular P3HT commercially purchased from Aldrich Chemical was also tested. In addition to the low HOMO

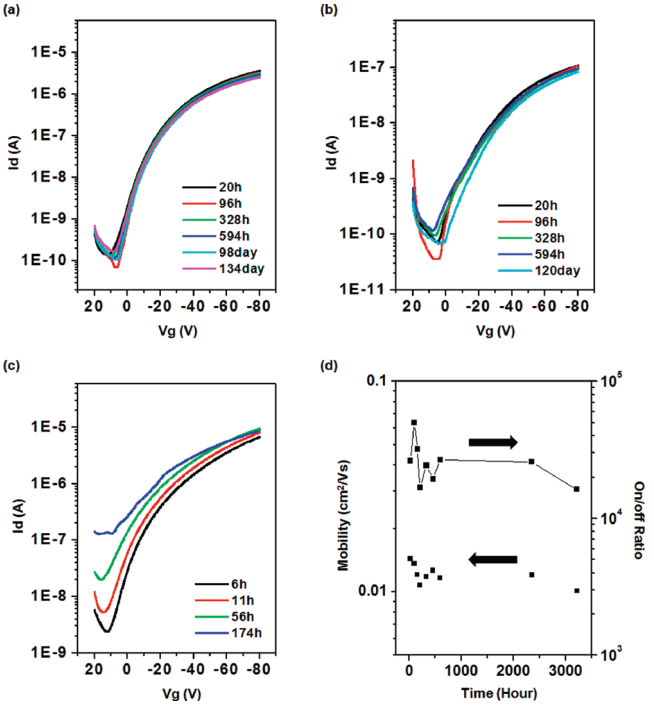

Figure 7. Stability of OFET devices: transfer curves after exposure to ambient air for (a) PDTST, (b) PDTQT, and (c) P3HT. (d) Change in mobility and on/off ratios for PDTST.

level, because the end-capping units were substituted at the terminal thiophene group, as described in the Synthesis section,[9] high air-stability was observed. In contrast with the poor air stability in P3HT shown as Figure 7c, no degradation in performance was observed after 30 days of exposure to air (Figure 7). Even after 90 days, the device retained >80% of its initial mobility, and the threshold voltages and on/off ratios were nearly the same as the initial values measured in PDTST. PDTQT also exhibited remarkable oxidative stability with a high oxidative potential.

In conclusion, we have modified two polythiophene derivatives to obtain extended π-conjugation in the side chain. PDTST and PDTQT showed high solubility and high performances as OFET devices, affording field effect mobilities of 0.050 and 0.003 $cm^2/(V\ s)$, respectively. Also, both polymers exhibited good oxidative stability over the course of 90 days of exposure, possibly made by the low HOMO levels derived from intramolecular repulsion. The advantages of these side-chain-modified polythiophene derivatives, with respect to FET performance and stability, suggest that these polymers represent a class of promising solution-processable polymeric semiconductors. Such side chain modifications are also expected to yield high solubility and oxidative stability as well as improved electrical performance when adopted in other semiconducting polymers.

Acknowledgment. This research was supported by a grant (F0004010-2009-32) from the Information Display R&D Center, and a grant from the Knowledge Economy Frontier R&D Program funded by the Ministry of Knowledge Economy of Korean Government, Basic Science Research Program through the National Research Foundation of Korea (NRF) funded by the Ministry of Education, Science and Technology (2009-0080273) and MKE and KIAT through the Workforce Development Program in Strategic Technology.

Supporting Information Available: TGA, in-plane GIXD patterns, and field effect mobility depended on the hydrophobicity of dielectric surfaces. This material is available free of charge via the Internet at http://pubs.acs.org.

References and Notes

(1) (a) Bao, Z.; Dodabalapur, A.; Lovinger, A. J. *Appl. Phys. Lett.* **1996**, *69*, 4108–4110. (b) Sirringhaus, H.; Tessler, N.; Friend, R. H. *Science* **1998**, *280*, 1741–1743. (c) Sirringhaus, H.; Brown, P. J.; Friend, R. H.; Nielsen, M. M.; Bechgaard, K.; Langeveld-Voss, B. M. W.; Spiering, A. J. H.; Janssen, R. A. J.; Meijer, E. W.; Herwig, P.; de Leeuw, D. M. *Nature* **1999**, *401*, 685–688. (d) Dimitrakopoulos, C. D.; Malenfant, P. R. L. *Adv. Mater.* **2002**, *14*, 99–117. (e) Salleo, A. *Mater. Today* **2007**, *10*, 38–45. (f) Miguel, L. S.; Matzger, A. J. *Macromolecules* **2007**, *40*, 9233–9237. (g) Yue, W.; Zhao, Y.; Tian, H.; Song, D.; Xie, Z.; Yan, D.; Geng, Y.; Wang, F. *Macromolecules* **2009**, *42*, 6510–6518. (h) Li, Y.; Kim, T. H.; Zhao, Q.; Kim, E. H.; Han, S. H.; Kim, Y. H.; Jang, J.; Kwon, S. K. *J. Polym. Sci., Part A: Polym. Chem.* **2008**, *46*, 5115–5122. (i) Chung, D. S.; Lee, S. J.; Park, J. W.; Choi, D. B.; Lee, D. H.; Park, J. W.; Shin, S. C.; Kim, Y. H.; Kwon, S. K.; Park, C. E. *Chem. Mater.* **2008**, *20*, 3450. (j) Ju, J. U.; Chung, D. S.; Kim, S. O.; Jung, S. O.; Park, C. E.; Kim, Y. H.; Kwon, S. K. *J. Polym. Sci., Polym. Chem.* **2009**, *47*, 1609. (k) Dang, T. T. M.; Park, S. J.; Park, J. W.; Chung, D. S.; Park, C. E.; Kim, Y. H.; Kwon, S. K. *J. Polym. Sci., Part A: Polym. Chem.* **2007**, *45*, 5277–5284.

(2) (a) Abdou, M. S. A.; Orfino, F. P.; Son, Y.; Holdcroft, S. *J. Am. Chem. Soc.* **1997**, *119*, 4518–4524. (b) Mattis, B. A.; Chang, P. C.; Subramanian, V. *Synth. Met.* **2006**, *156*, 1241–1248.

(3) (a) Ong, B. S.; Wu, Y.; Liu, P.; Gardner, S. *J. Am. Chem. Soc.* **2004**, *126*, 3378–3379. (b) Ong, B. S.; Wu, Y.; Li, Y.; Liu, P.; Pan, H. *Chem.—Eur. J.* **2008**, *14*, 4766–4778.

(4) (a) Sirringhaus, H.; Wilson, R. J.; Friend, R. H.; Inbasekaran, M.; Wu, W.; Woo, E. P.; Grell, M.; Bradley, D. D. C. *Appl. Phys. Lett.* **2000**, *77*, 406–408. (b) McCulloch, I.; Heeney, M.; Bailey, C.; Genevicius, K.; Macronald, I.; Shkunov, M.; Sparrowe, D.; Tierney, S.; Wagner, R.; Zhang, W.; Chabinyc, M. L.; Kline, R. J.; Mcgehee, M. D.; Toney, M. F. *Nat. Mater.* **2006**, *5*, 328–333.

(5) Ong, B. S.; Li, Y.; Wu, Y.; Liu, P.; Birau, M.; Pan, H. *Adv. Mater.* **2006**, *18*, 3029–3032.

(6) (a) Bao, Z.; Lovinger, A. J. *Chem. Mater.* **1999**, *11*, 2607–2612. (b) McCullough, R. D.; Exbank, P. C.; Loewe, R. S. *J. Am. Chem. Soc.* **1997**, *119*, 633–634. (c) Langeveld-Voss, B. M. W.; Janssen, R. A. J.; Christiaans, M. P. T.; Meskers, S. C. J.; Dekkers, H. P. J. M.; Meijer, E. W. *J. Am. Chem. Soc.* **1996**, *118*, 4908–4909. (d) Li, Y.; Yang, H.; Cheng, Y.; Pomerantz, M. *Macromolecules* **1995**, *28*, 5706–5708. (e) Vamvounis, G.; Holdcroft, S. *Macromolecules* **2001**, *34*, 141–143. (f) Zhou, E.; Tan, Z.; He, Y.; Yang, C.; Li, Y. *J. Polym. Sci,. Part A: Polym. Chem.* **2007**, *45*, 629–638.

(7) (a) Hou, J.; Li, Y.; He, C.; Yang, C. *Chem. Commun.* **2006**, 871–873. (b) Hou, J.; Tan, Z.; Yan, Y.; He, Y.; Yang, C.; Li, Y. *J. Am. Chem. Soc.* **2006**, *128*, 4911–4916.

(8) Yu, C. Y.; Ko, B. T.; Ting, C.; Chen, C. P. *Sol. Energy Mater. Sol. Cells* **2009**, *93*, 613–620.

(9) (a) Wakamiya, A.; Yamazaki, D.; Nishinaga, T.; Kitagawa, T.; Komatsu, K. *J. Org. Chem.* **2003**, *68*, 8305–8314. (b) Turbiez, M.; Frère, P.; Roncali, F. *J. Org. Chem.* **2003**, *68*, 5357–5360. (c) Yanying Zhanga, Y.; Ichikawa, M.; Hattori, J.; Kato, T.; Sazaki, A.; Kanazawa, S.; Kato, S.; Zhang, C.; Taniguchi, Y. *Synth. Met.* **2009**, *159*, 1890–1895.

(10) Lu, K.; Di, C.; Xi, H.; Liu, Y.; Yu, G.; Qiu, W.; Zhang, H.; Gao, X.; Liu, Y.; Qi, T.; Du, C.; Zhu, D. *J. Mater. Chem.* **2008**, *18*, 3426–3432.

(11) (a) Chen, T.; Wu, X.; Rieke, R. D. *J. Am. Chem. Soc.* **1995**, *117*, 233–244. (b) Asadi, K.; Gholamrezais, F.; Smiths, E. C. P.; Blom, P. W. M.; Boer, B. D. *J. Mater. Chem.* **2007**, *17*, 1947–1953.

(12) Mozer, A. J.; Sariciftci, N. S.; Pivrikas, A.; Österbacka, R.; Juška, G.; Brassat, L.; Bässler, H. *Phys. Rev. B* **2005**, *71*, 035214.